EUROGRAPHICS 2021 / N. Mitra and I. Viola
(Guest Editors)

Volume 40 (2021), Number 2

Supplementary Material: Local Light Alignment for Multi-Scale Shape Depiction

Nolan Mestres[1] Romain Vergne[1] Camille Noûs[2] Joëlle Thollot[1]

[1] Univ. Grenoble Alpes, CNRS, Inria, Grenoble INP, LJK
[2] Cogitamus Laboratory

1. Introduction

In this supplementary document, we provide more examples of the light-shape congruency measurements found in Section 7 (Results and discussion) of the main paper. We perform this analysis on various models using different directions of light and different BRDF.

2. Figures

References

[RBD06] RUSINKIEWICZ S., BURNS M., DECARLO D.: Exaggerated shading for depicting shape and detail. *ACM Trans. Graph. 25*, 3 (July 2006), 1199–1205. URL: http://doi.acm.org/10.1145/1141911.1142015, doi:10.1145/1141911.1142015. 4, 5, 6, 9, 10, 13, 14, 17, 18, 21, 22, 25, 26

[VPB*09] VERGNE R., PACANOWSKI R., BARLA P., GRANIER X., SCHLICK C.: Light Warping for Enhanced Surface Depiction. *ACM Transactions on Graphics 28*, 3 (July 2009), 25:1–25:8. URL: https://hal.inria.fr/inria-00400829, doi:10.1145/1531326.1531331. 4, 5, 6, 7, 8, 9, 10, 11, 12, 13, 14, 15, 16, 17, 18, 19, 20, 21, 22, 23, 24, 25, 26, 27, 28

[VPB*11] VERGNE R., PACANOWSKI R., BARLA P., GRANIER X., SCHLICK C.: Improving Shape Depiction under Arbitrary Rendering. *IEEE Transactions on Visualization and Computer Graphics 17*, 8 (June 2011), 1071 – 1081. URL: https://hal.inria.fr/inria-00585144, doi:10.1109/TVCG.2010.252. 4, 5, 6, 7, 8, 9, 10, 11, 12, 13, 14, 15, 16, 17, 18, 19, 20, 21, 22, 23, 24, 25, 26, 27, 28

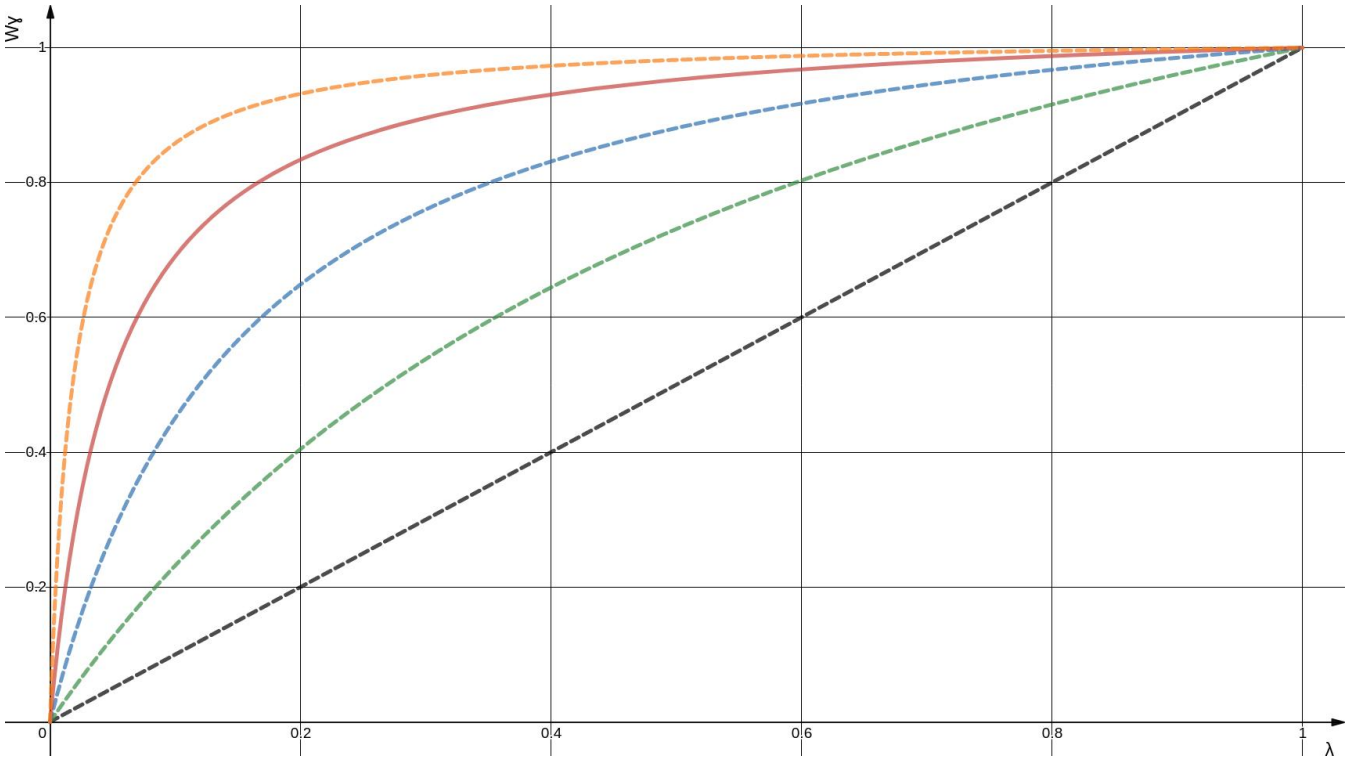

Figure 1: $W_\gamma(\lambda)$, the function used to remap confidence values λ_1 and λ_2, plotted with $\gamma = \{0, 1, 2, 3, 4\}$. As soon as $\lambda = \lambda_1 \cdot \lambda_2$ deviates from zero, we rotate the light. In practice a value of $\gamma = 3$ (red, continuous) is a good compromise between a qualitative shape depiction enhancement and no visible discontinuities.

Figure 2: More detailed version of Figure 7. Enhancements at arbitrary detail scales. Each column shows a different value of σ. The coarsest scale enhances the overall shape while finer scales enhance smaller details of the model.

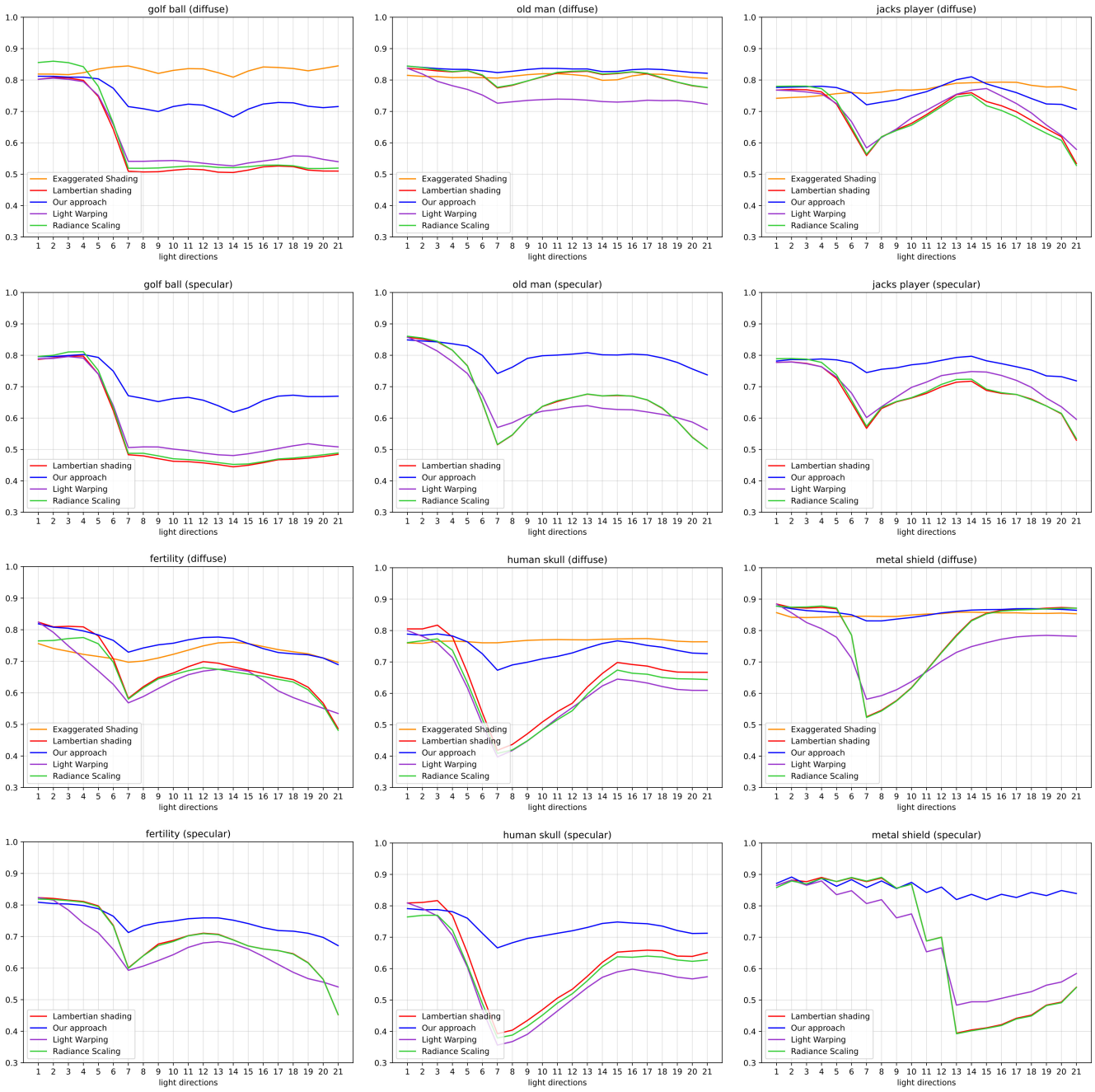

Figure 3: Average congruence scores obtained on various models using previous work techniques and our method. Renderings and scores are shown in Figures 4 to 27. The first and third rows present the scores obtained using a diffuse model, while the second and fourth rows display the specular results on the same models. Our enhancement better aligns shape and shading flows while it also increases magnitudes of the flows, leading to an overall better score. It solves most masking effects while keeping a coherent appearance with respect to the shading without enhancement. Note that Exaggerated Shading [RBD06] obtains sometimes a better score; this is mainly due to its use of a half-Lambertian shading model that solves all masking effects, at the cost of an impaired material appearance and a global direction of light that becomes difficult to understand (see the renderings in the following figures). For specular scenarios we compared against Light Warping [VPB*09] and Radiance Scaling [VPB*11] only, as Exaggerated Shading uses a custom half-Lambertian shading model.

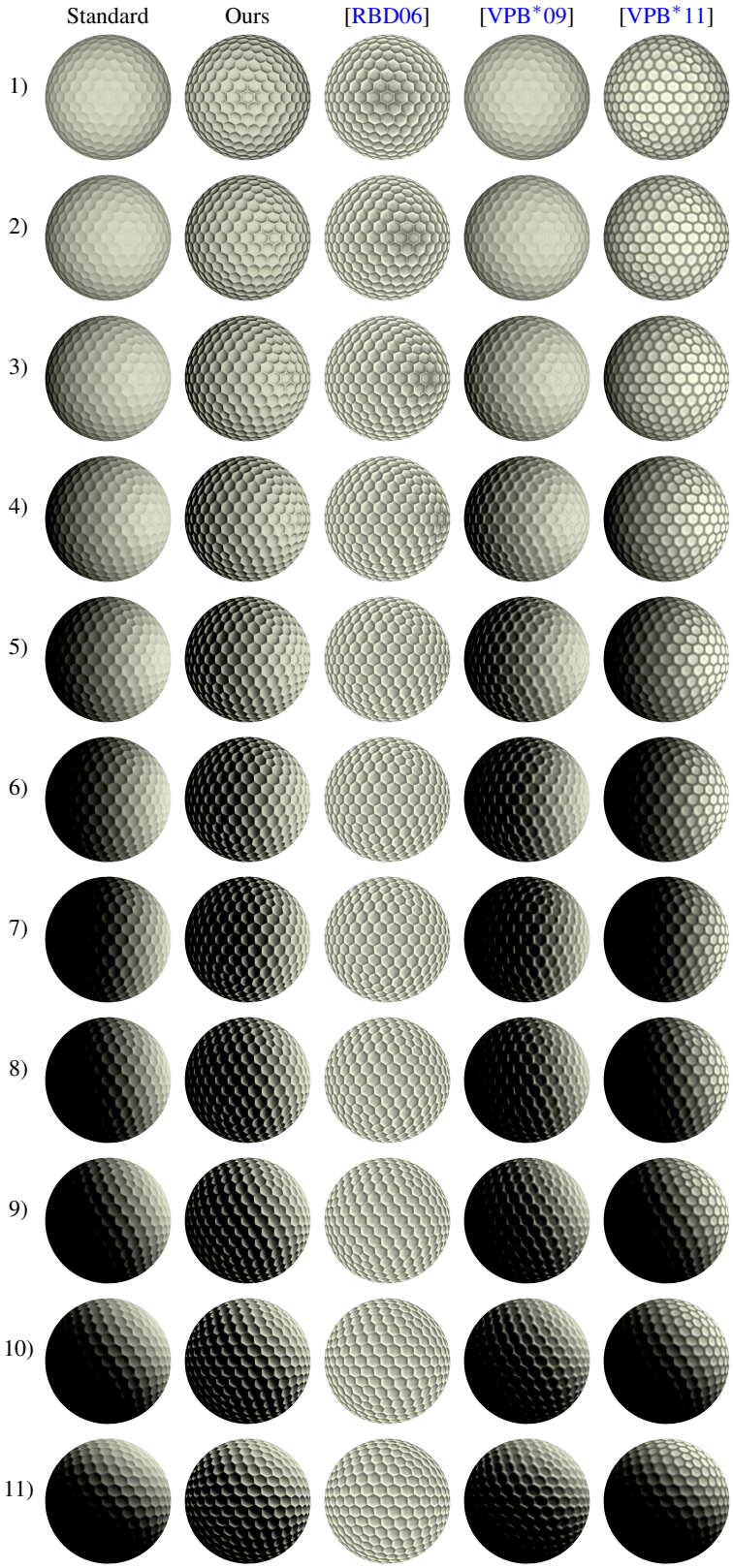

Figure 4: Golf ball, Oren-Nayar 1/2. Each row corresponds to a different direction of light as numbered in the paper (from 1 to 21).

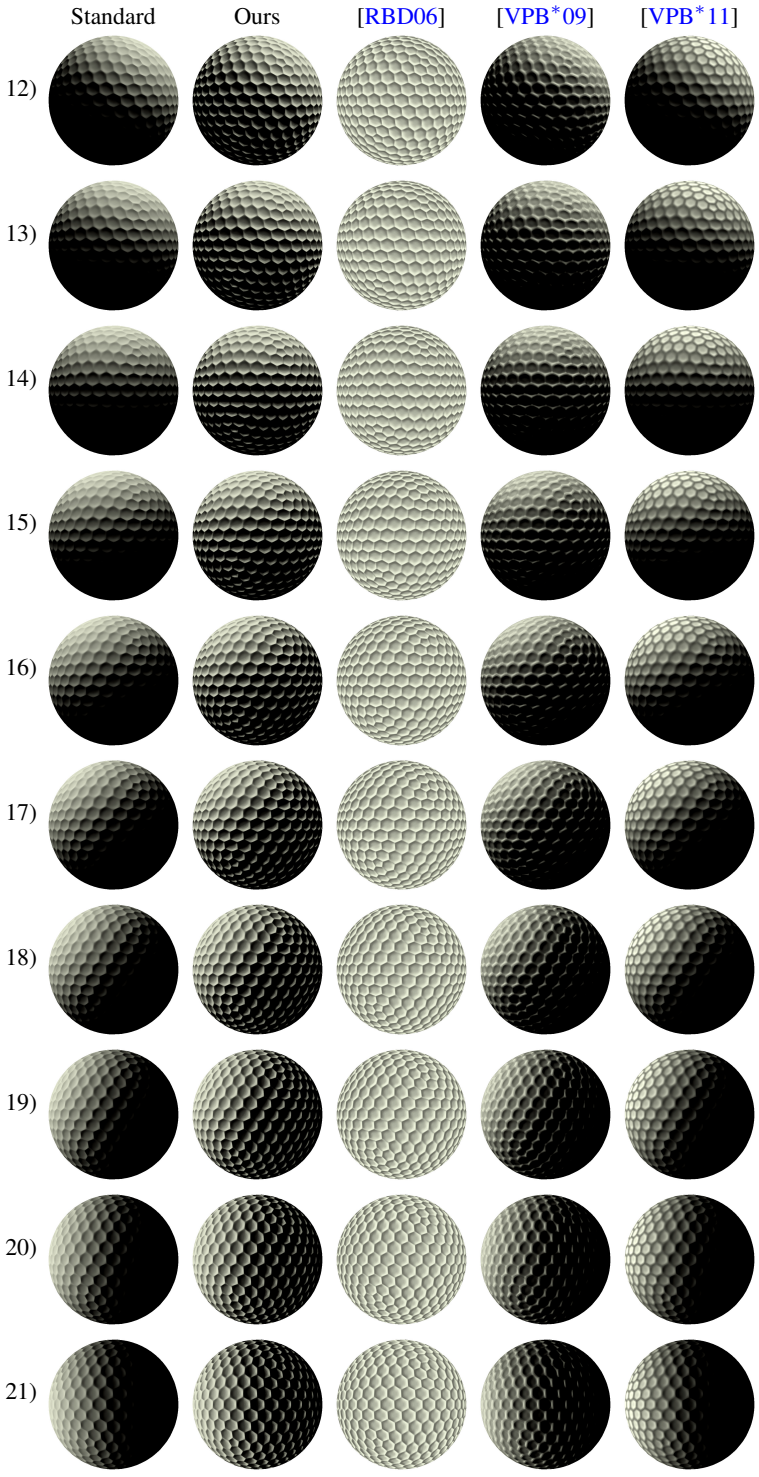

Figure 5: Golf ball, Oren-Nayar 2/2. Each row corresponds to a different direction of light as numbered in the paper (from 1 to 21).

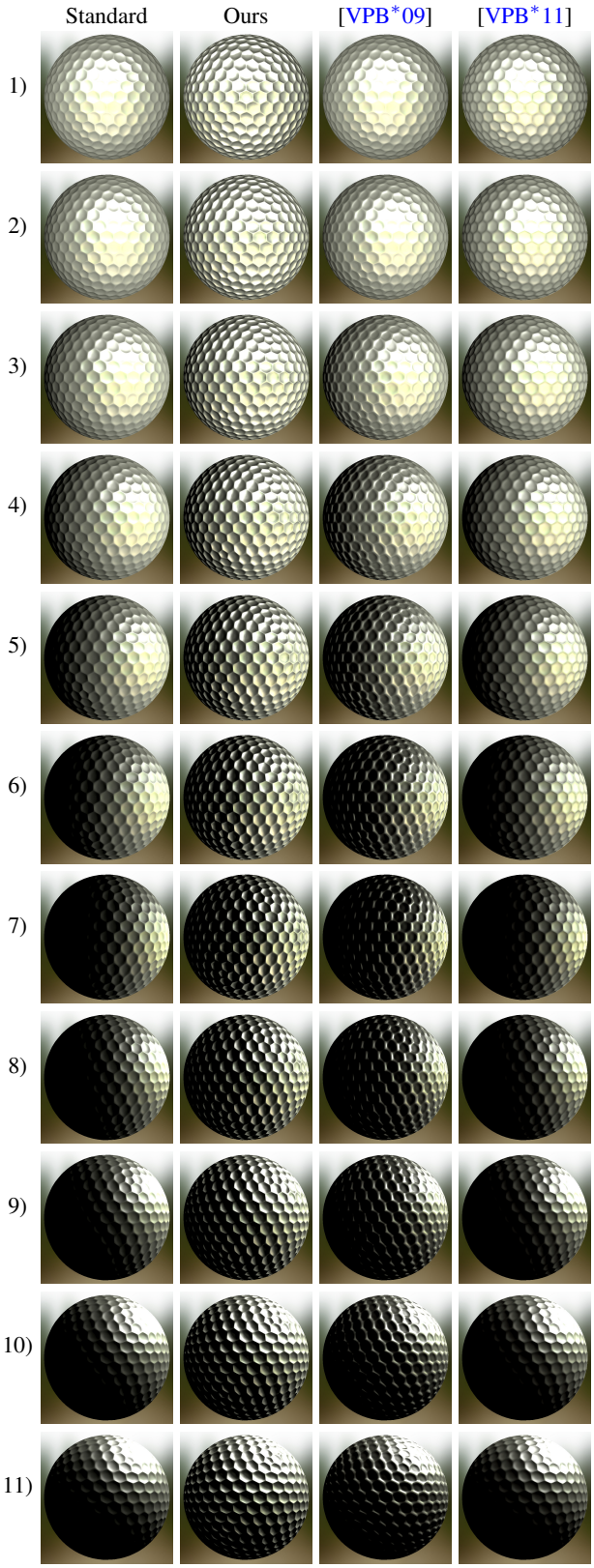

Figure 6: Golf ball, Cook-Torrance 1/2. Each row corresponds to a different direction of light as numbered in the paper (from 1 to 21).

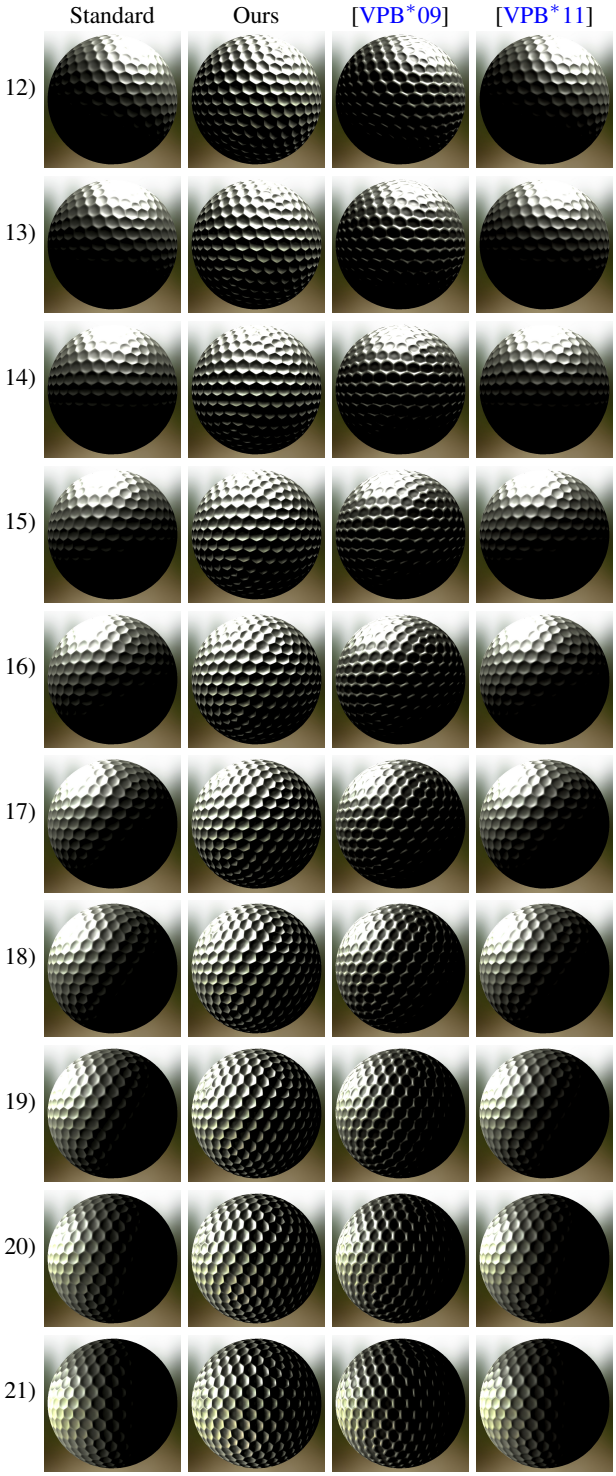

Figure 7: Golf ball, Cook-Torrance 2/2. Each row corresponds to a different direction of light as numbered in the paper (from 1 to 21).

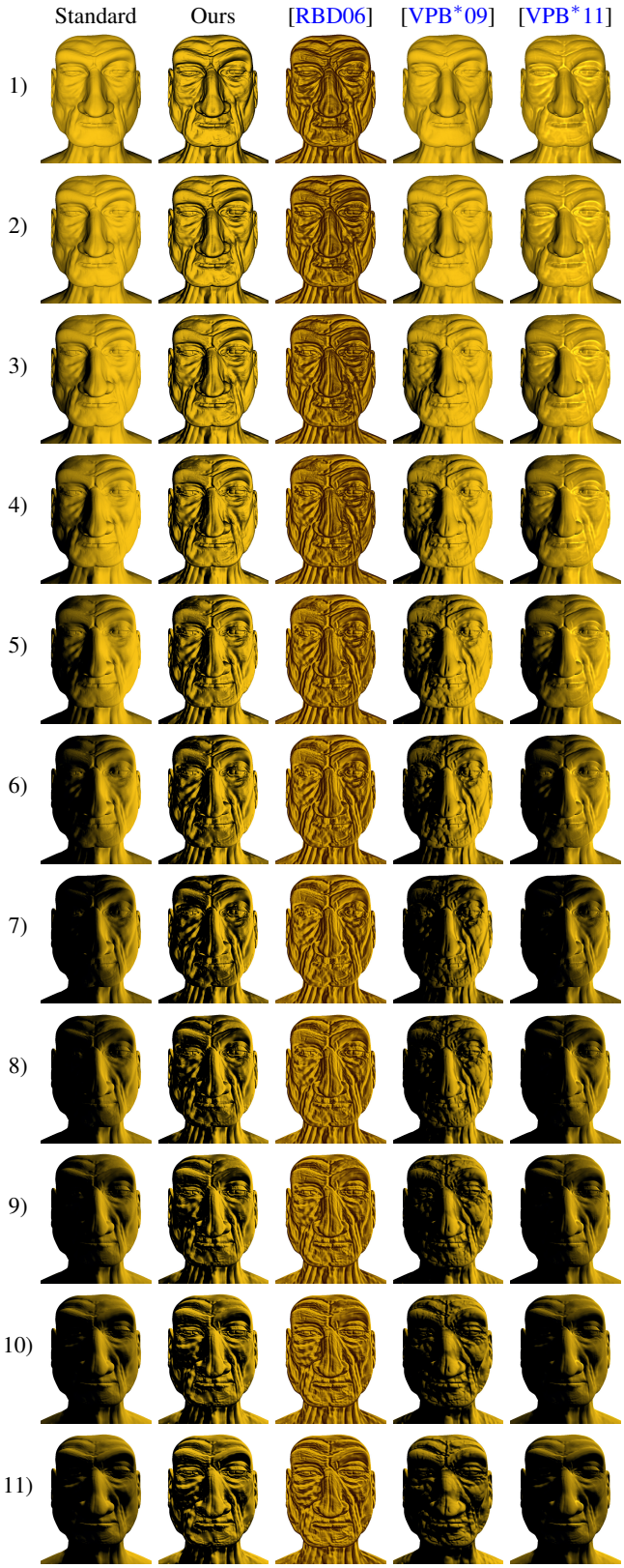

Figure 8: Old man, Oren-Nayar 1/2. Each row corresponds to a different direction of light as numbered in the paper (from 1 to 21).

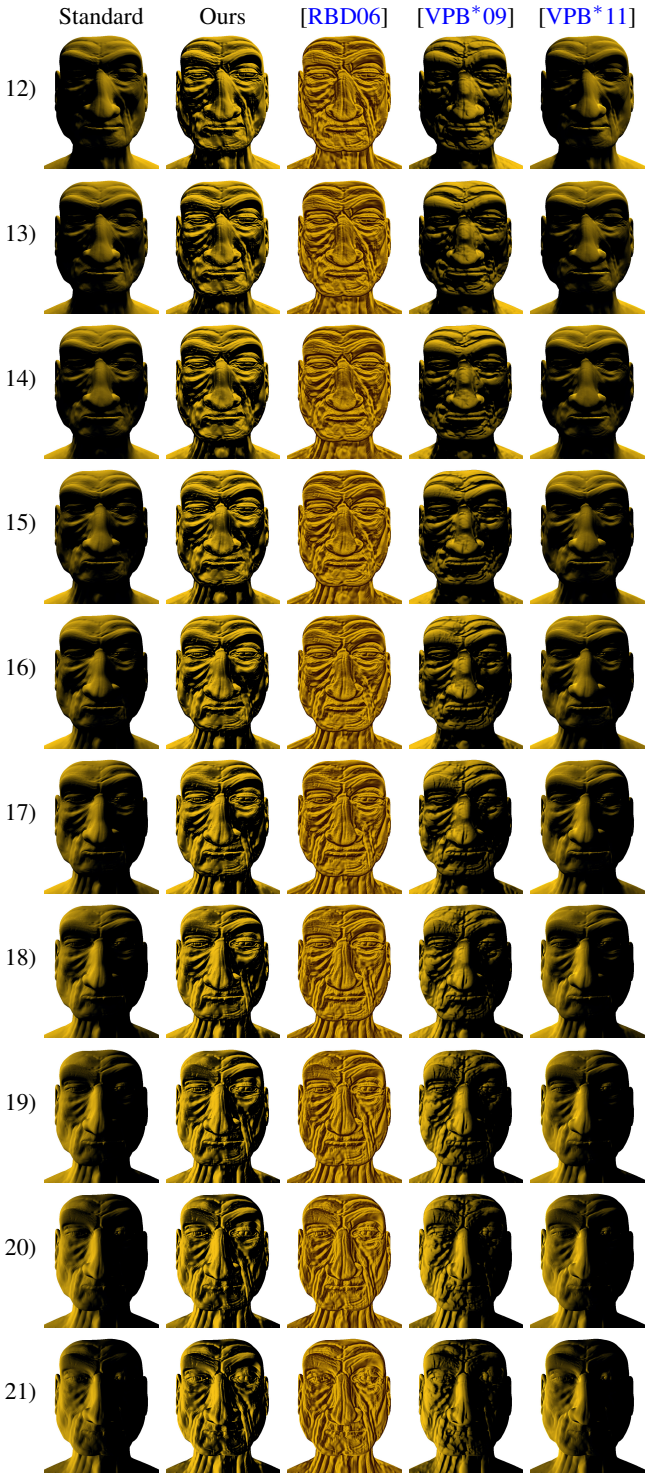

Figure 9: Old man, Oren-Nayar 2/2. Each row corresponds to a different direction of light as numbered in the paper (from 1 to 21).

Figure 10: Old man, Cook-Torrance 1/2. Each row corresponds to a different direction of light as numbered in the paper (from 1 to 21).

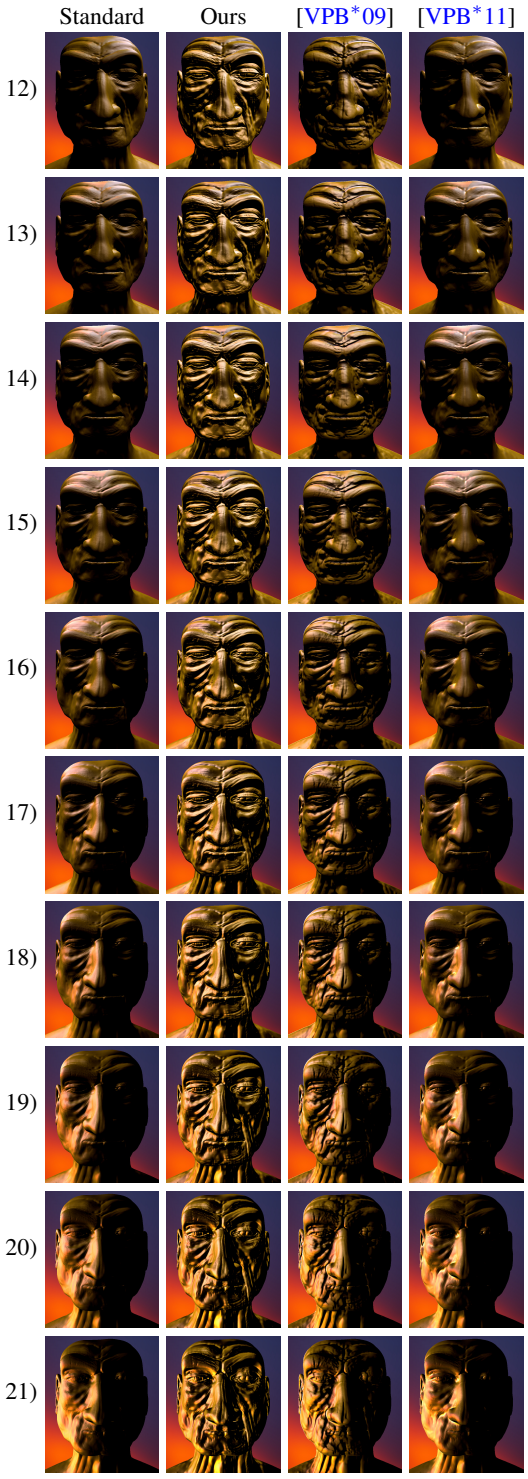

Figure 11: Old man, Cook-Torrance 2/2. Each row corresponds to a different direction of light as numbered in the paper (from 1 to 21).

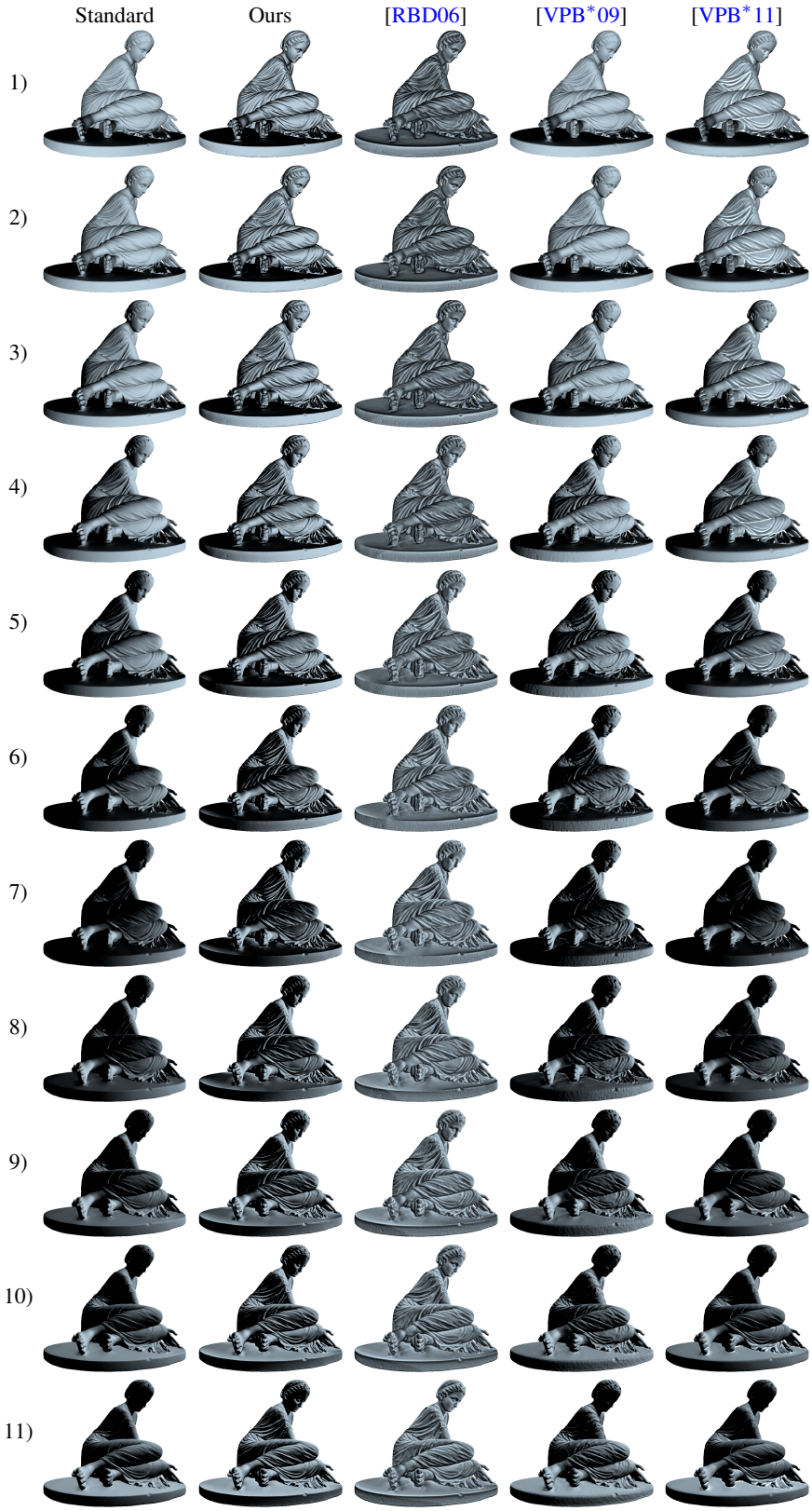

Figure 12: Jacks player, Oren-Nayar 1/2. Each row corresponds to a different direction of light as numbered in the paper (from 1 to 21).

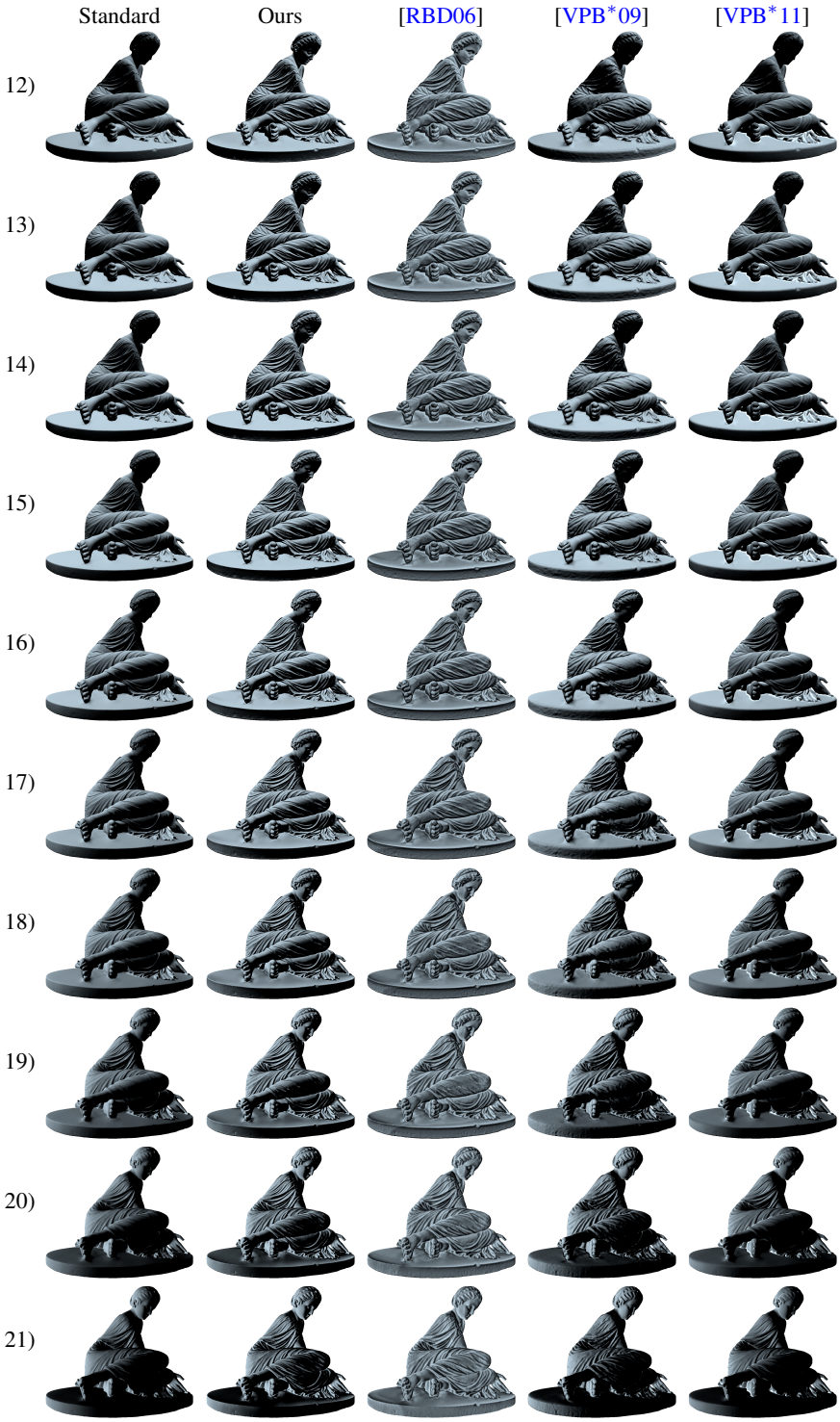

Figure 13: Jacks player, Oren-Nayar 2/2. Each row corresponds to a different direction of light as numbered in the paper (from 1 to 21).

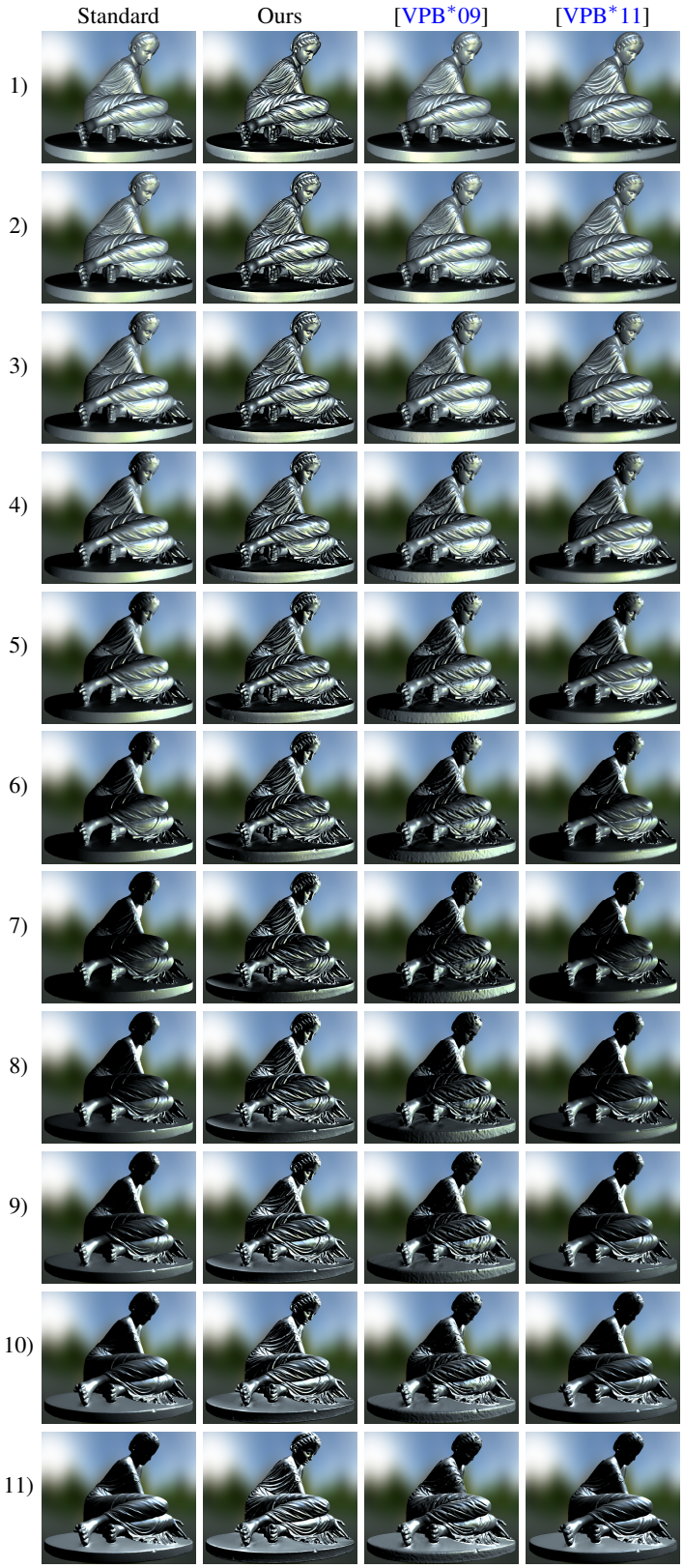

Figure 14: Jacks player, Cook-Torrance 1/2. Each row corresponds to a different direction of light as numbered in the paper (from 1 to 21).

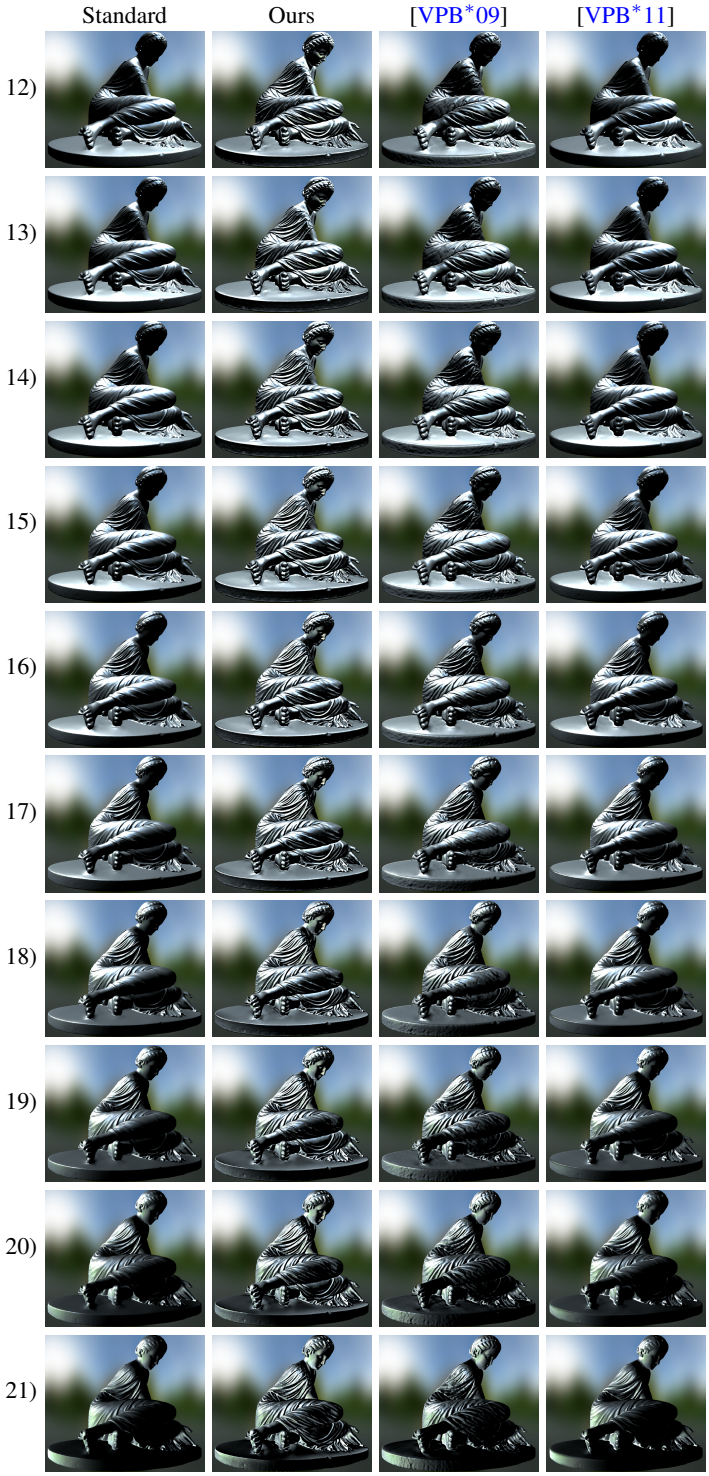

Figure 15: Jacks player, Cook-Torrance 2/2. Each row corresponds to a different direction of light as numbered in the paper (from 1 to 21).

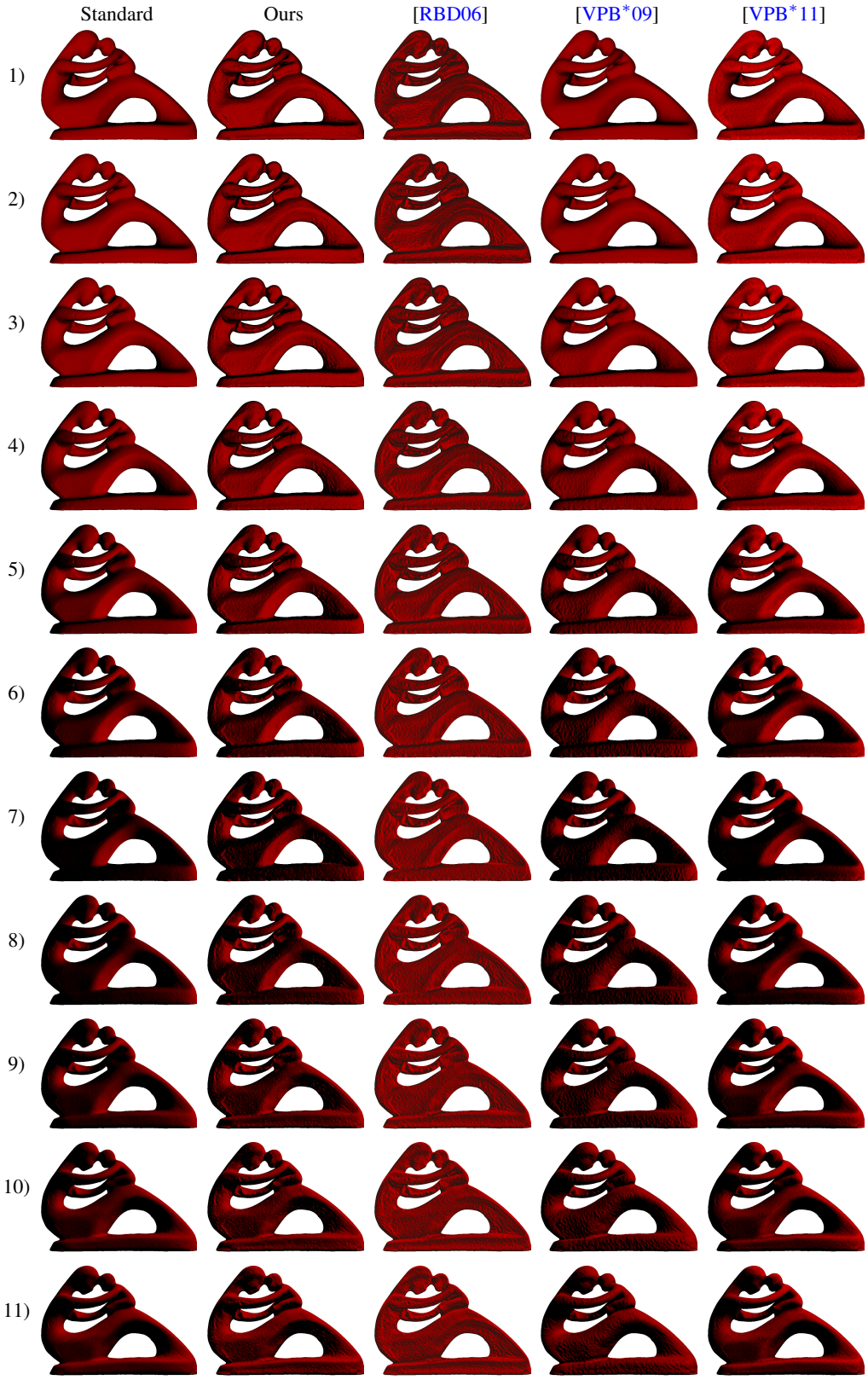

Figure 16: Fertility model, Oren-Nayar 1/2. Each row corresponds to a different direction of light as numbered in the paper (from 1 to 21).

Figure 17: Fertility model, Oren-Nayar 2/2. Each row corresponds to a different direction of light as numbered in the paper (from 1 to 21).

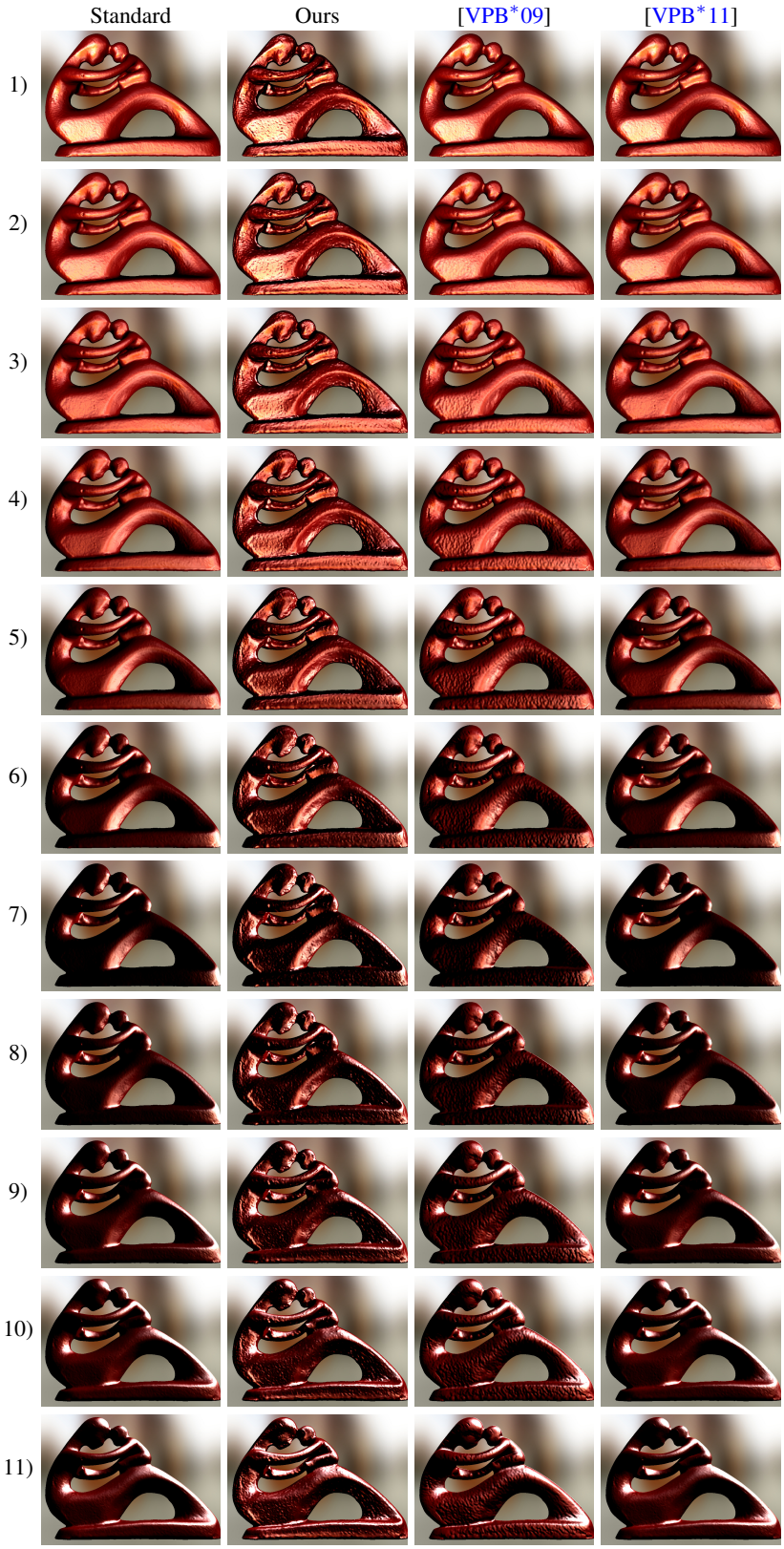

Figure 18: Fertility model, Cook-Torrance 1/2. Each row corresponds to a different direction of light as numbered in the paper (from 1 to 21).

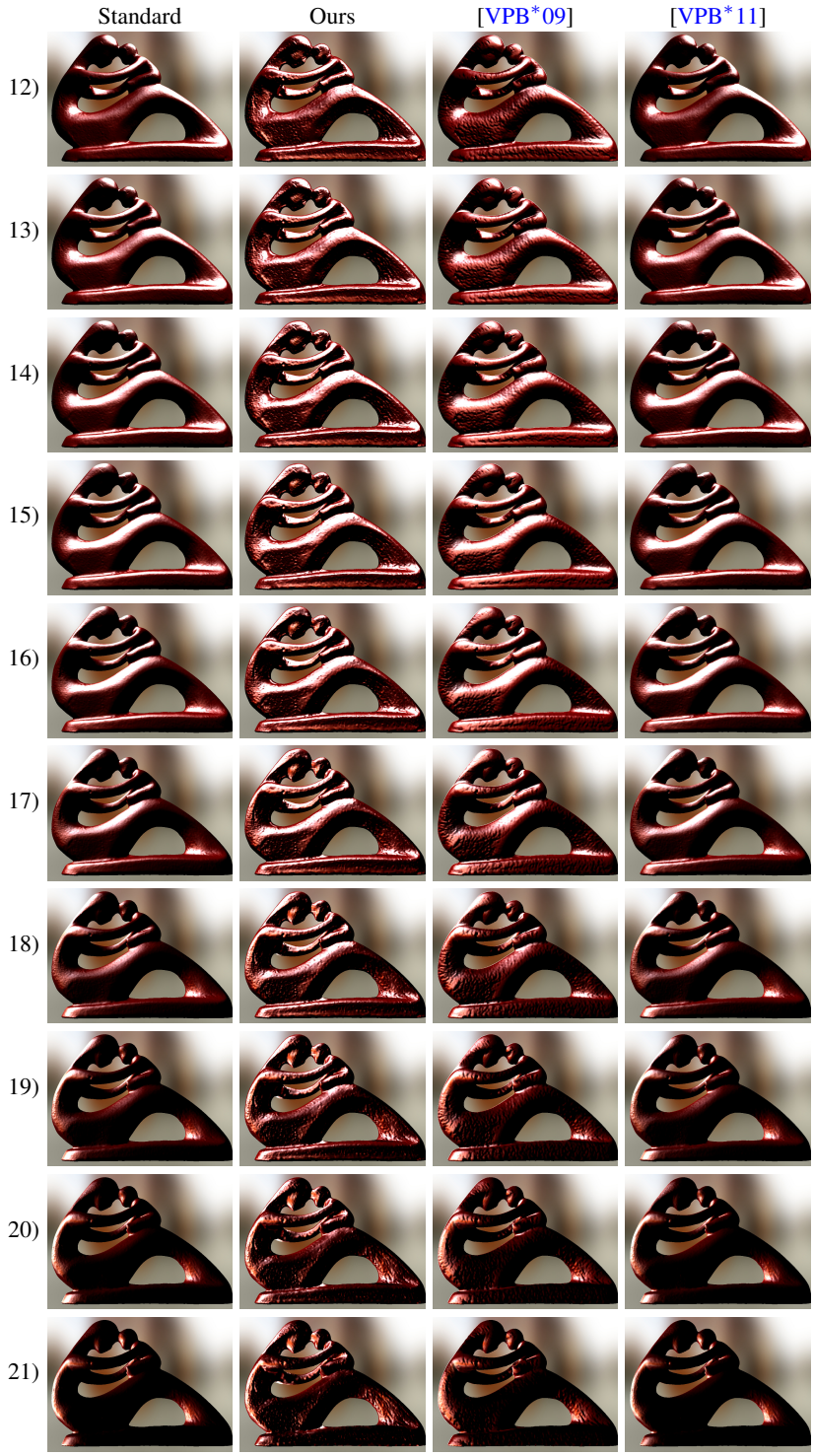

Figure 19: Fertility model, Cook-Torrance 2/2. Each row corresponds to a different direction of light as numbered in the paper (from 1 to 21).

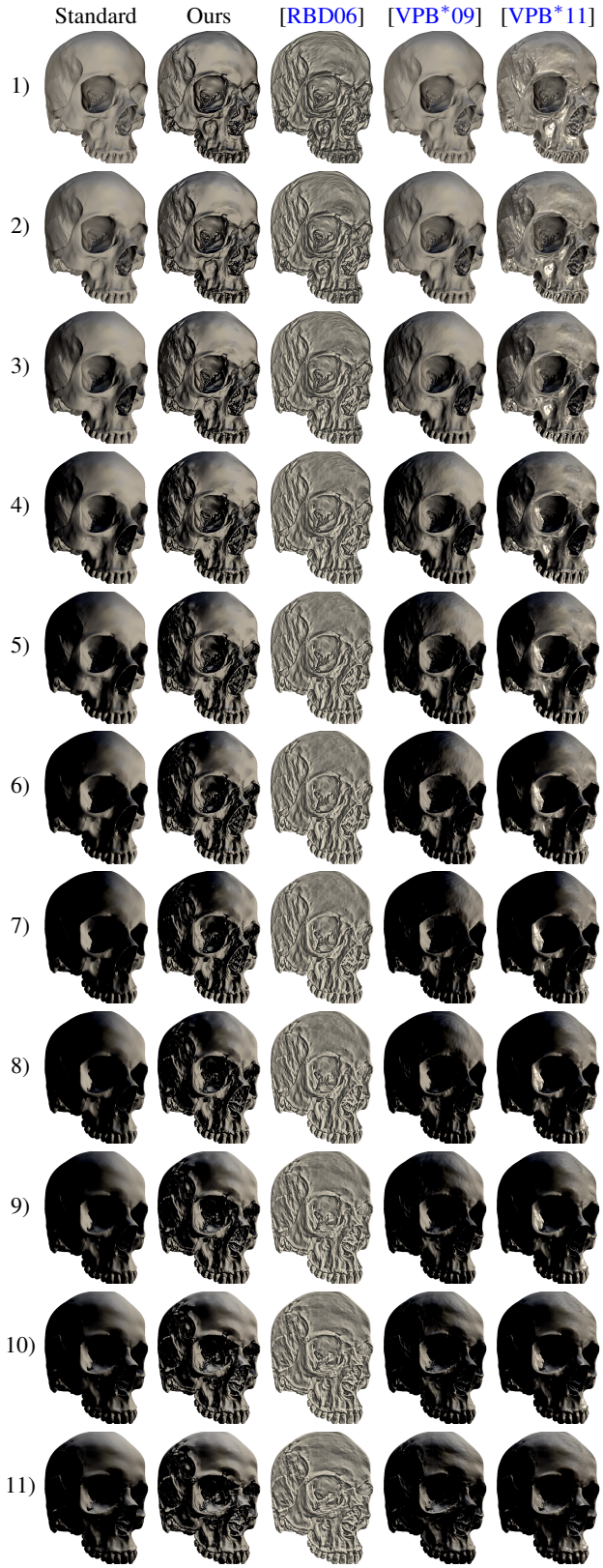

Figure 20: Human skull, Oren-Nayar 1/2. Each row corresponds to a different direction of light as numbered in the paper (from 1 to 21).

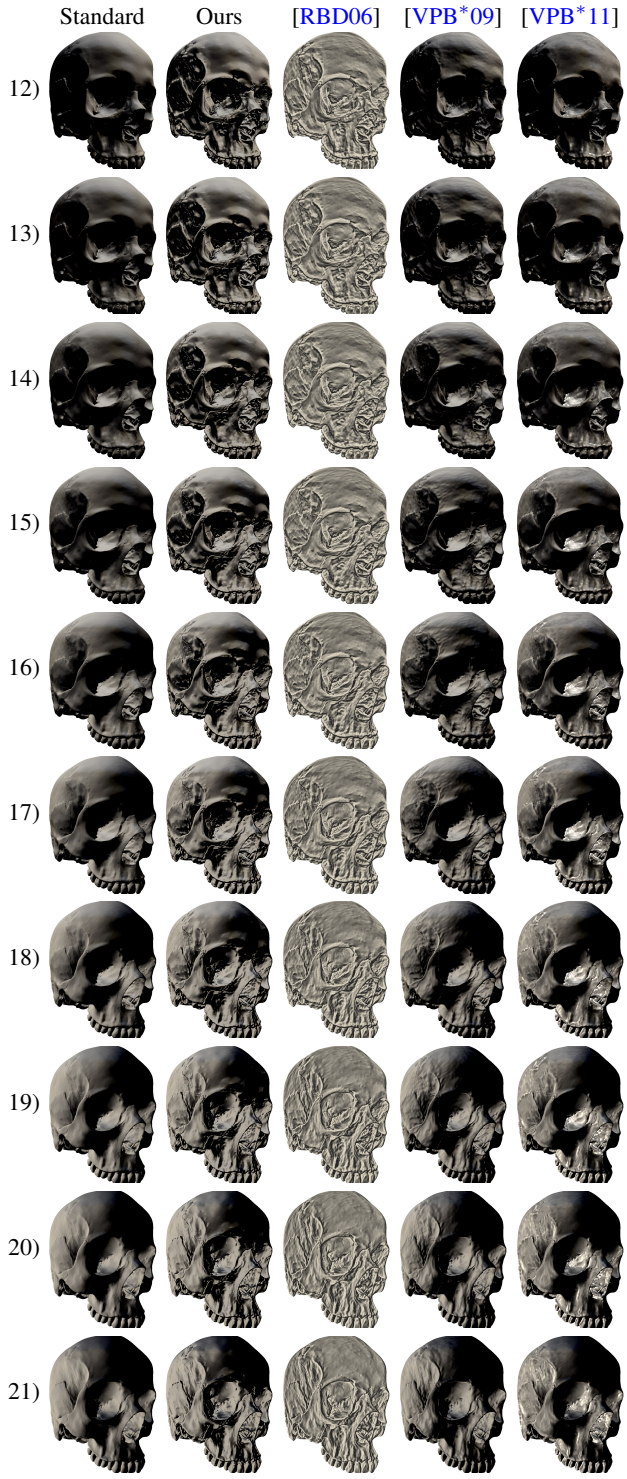

Figure 21: Human skull, Oren-Nayar 2/2. Each row corresponds to a different direction of light as numbered in the paper (from 1 to 21).

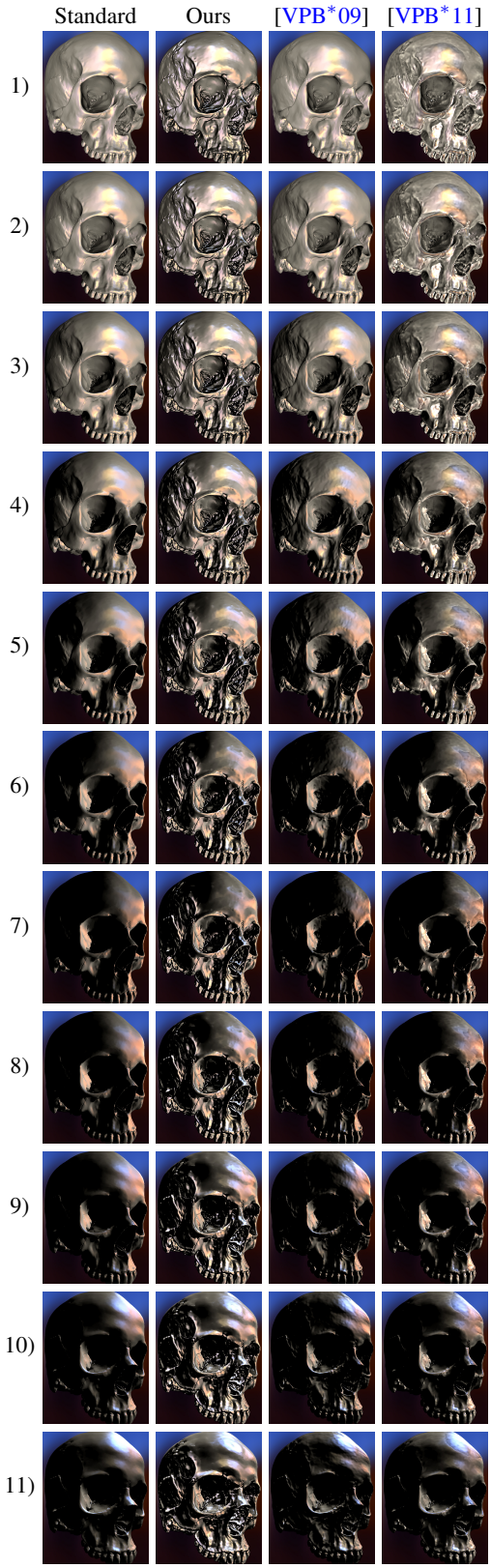

Figure 22: Human skull, Cook-Torrance 1/2. Each row corresponds to a different direction of light as numbered in the paper (from 1 to 21).

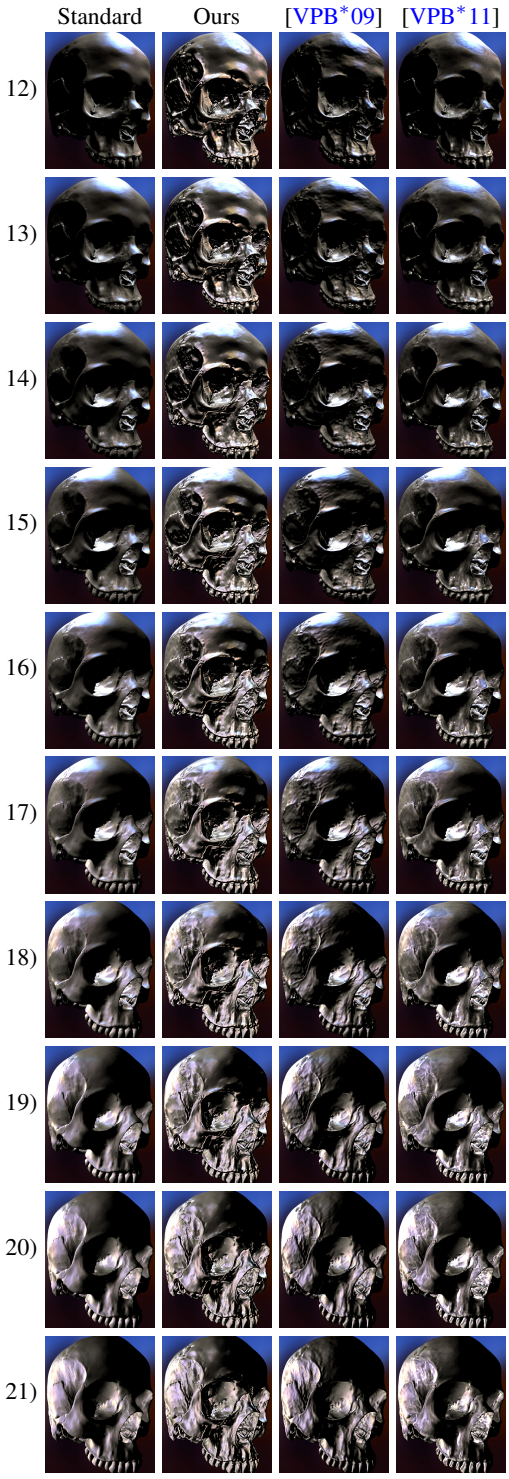

Figure 23: Human skull, Cook-Torrance 2/2. Each row corresponds to a different direction of light as numbered in the paper (from 1 to 21).

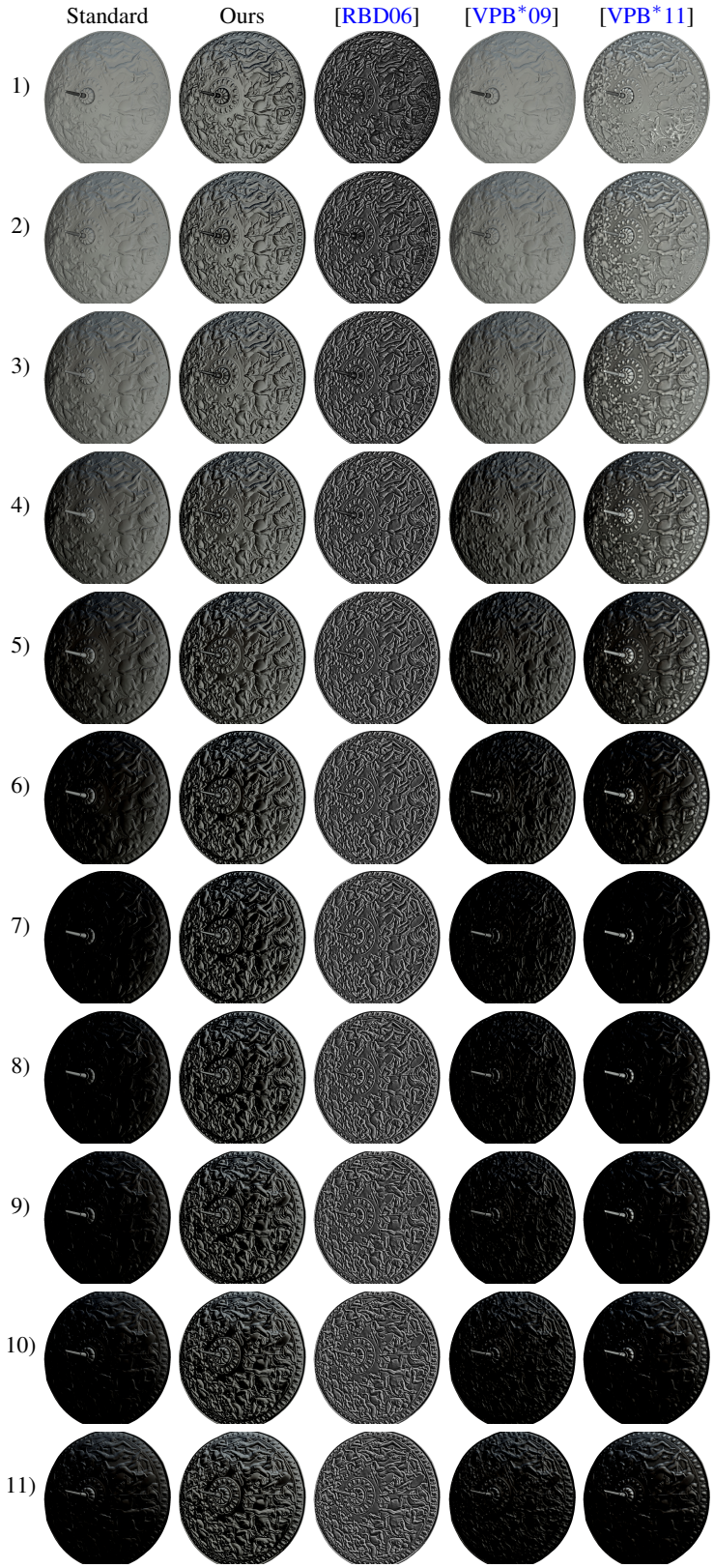

Figure 24: Metal shield, Oren-Nayar 1/2. Each row corresponds to a different direction of light as numbered in the paper (from 1 to 21).

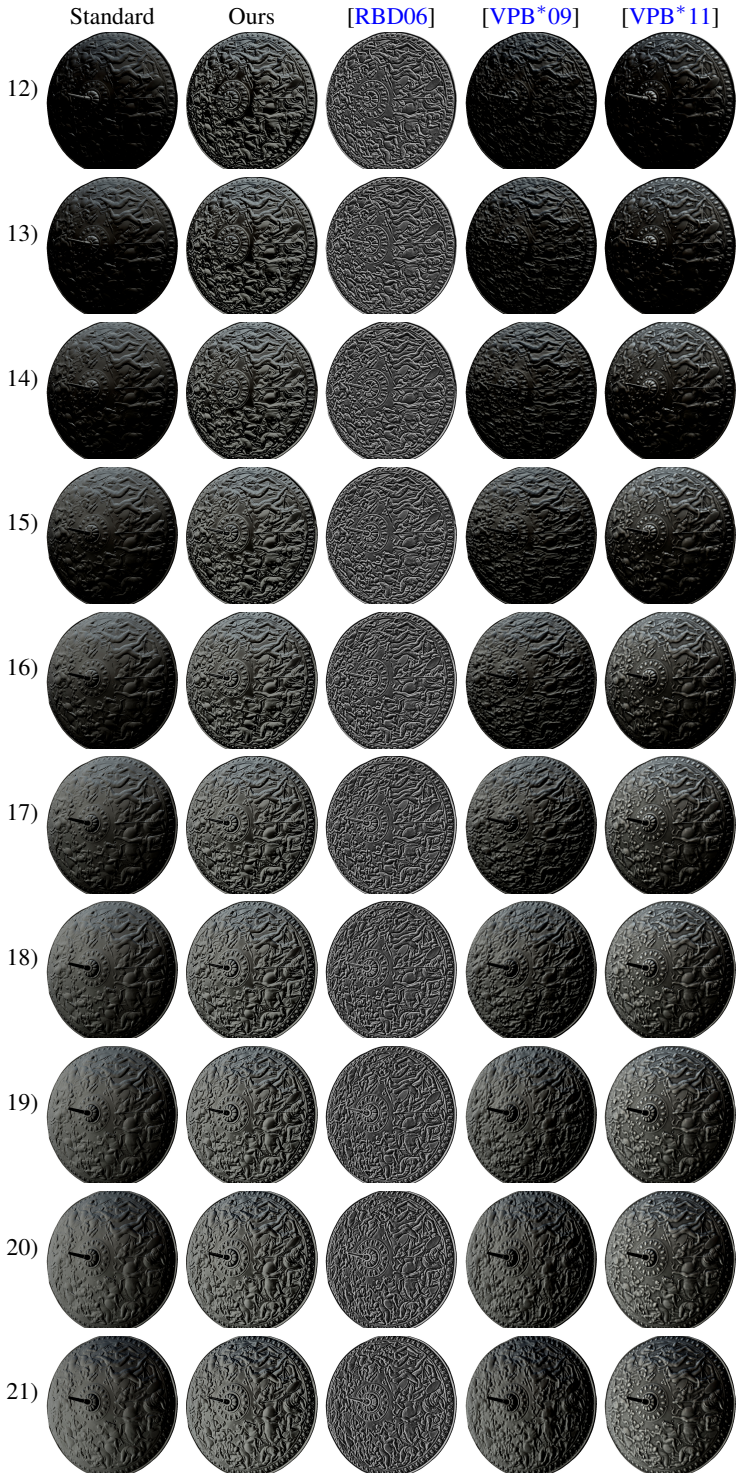

Figure 25: Metal shield, Oren-Nayar 2/2. Each row corresponds to a different direction of light as numbered in the paper (from 1 to 21).

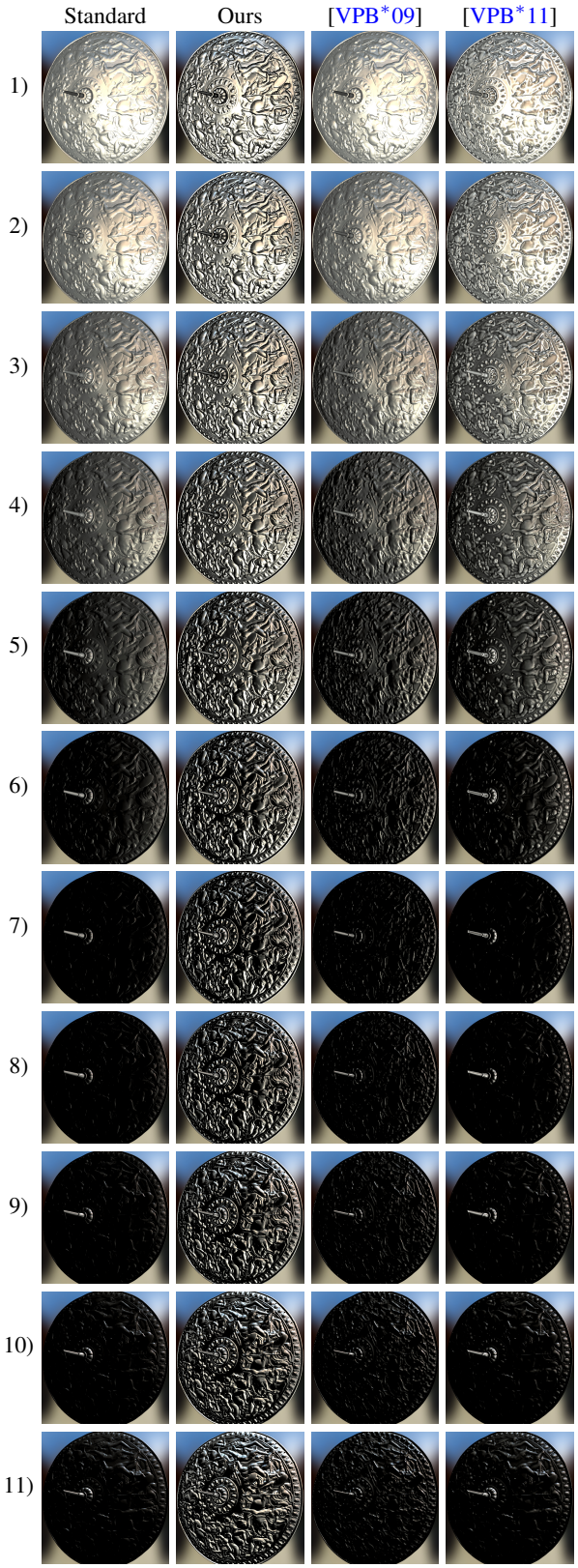

Figure 26: Metal shield, Cook-Torrance 1/2. Each row corresponds to a different direction of light as numbered in the paper (from 1 to 21).

Figure 27: Metal shield, Cook-Torrance 2/2. Each row corresponds to a different direction of light as numbered in the paper (from 1 to 21).